Published in final edited form as:
Mol Cancer Ther. 2015 January ; 14(1): 141–150. doi:10.1158/1535-7163.MCT-14-0658.

Near infrared photoimmunotherapy in the treatment of disseminated peritoneal ovarian cancer

Kazuhide Sato, **Hirofumi Hanaoka**, **Rira Watanabe**, **Takahito Nakajima**, **Peter L. Choyke**, and **Hisataka Kobayashi***
Molecular Imaging Program, Center for Cancer Research, National Cancer Institute/NIH

Abstract

Near infrared photoimmunotherapy (NIR-PIT) is a new cancer treatment that combines the specificity of intravenously injected antibodies for targeting tumors with the toxicity induced by photosensitizers after exposure to near infrared (NIR) light. Herein, we evaluate the efficacy of NIR-PIT in a mouse model of disseminated peritoneal ovarian cancer. *In vitro* and *in vivo* experiments were conducted with a HER2-expressing, luciferase expressing, ovarian cancer cell line (SKOV-luc). An antibody-photosensitizer conjugate (APC) consisting of trastuzumab and a phthalocyanine dye, IRDye-700DX, was synthesized (tra-IR700) and cells or tumors were exposed to near infrared (NIR) light. *In vitro* PIT cytotoxicity was assessed with dead staining and luciferase activity in freely growing cells and in a 3D spheroid model. *In vivo* NIR-PIT was performed in mice with tumors implanted in the peritoneum and in the flank and these assessed by tumor volume and/or bioluminescence. *In vitro* NIR-PIT-induced cytotoxicity was light dose dependent. Repeated light exposures induced complete tumor cell killing in the 3D spheroid model. *In vivo* the anti-tumor effects of NIR-PIT were confirmed by significant reductions in both tumor volume and luciferase activity in the flank model (NIR-PIT vs control in tumor volume changes at day 10; p=0.0001, NIR-PIT vs control in luciferase activity at day 4; p=0.0237), and the peritoneal model (NIR-PIT vs control in luciferase activity at day 7; p=0.0037). NIR-PIT provided effective cell killing in this HER2 positive model of disseminated peritoneal ovarian cancer. Thus, NIR-PIT is a promising new therapy for the treatment of disseminated peritoneal tumors.

Keywords

photoimmunotherapy; bioluminescence; epidermal growth factor receptor; ovarian cancer; disseminated peritoneal model

Introduction

Ovarian carcinoma affected approximately 22,000 new patients in the United States in 2012 and resulted in approximately 14,000 deaths (1). Ovarian adenocarcinoma is responsible for at least 90% of all ovarian malignancies and it is the second most frequent gynecologic

*Corresponding author: Hisataka Kobayashi, M.D., Ph.D., Molecular Imaging Program, Center for Cancer Research, National Cancer Institute, NIH, Building 10, RoomB3B69, MSC1088, Bethesda, MD 20892-1088. Phone: 301-435-4086, Fax: 301-402-3191. Kobayash@mail.nih.gov.

malignancy after cervical cancer. Despite various attempts to screen and detect ovarian carcinoma early, over 85% of patients present at an advanced stage which commonly consists of nodal and intraperitoneal dissemination (2). While overall 5 year survival over the last 3 decades has improved from 37% to 46% with a combination of radical surgery and cytotoxic chemotherapy, ovarian cancer remains a major cause of morbidity and mortality for women throughout the world (2,3). The reasons for this are complex but principally involve the inherent difficulty of safely removing all cancer implants from the peritoneum and the relatively rapid onset of chemo-resistance in advanced stage ovarian cancer (4). Therefore, there is an urgent need for improved ovarian cancer therapies that are highly effective yet cause minimal damage to adjacent normal tissue (5).

The concept of using targeted light therapy is over three decades old (6). Due to the hydrophobicity of traditional photodynamic therapy (PDT) sensitizers, the pharmacokinetics of antibody conjugated PDT agents limits its selective targeting ability. Therefore, PDT sensitizers targeting with antibodies was only successful in intratumoral or intraperitoneal preclinical models (7). The recognition that a hydrophilic phthalocyanine-based photosensitizer could be conjugated to an antibody and exposed to near infrared (NIR) light has led to a new method to treat tumors with light. This NIR photoimmunotherapy (NIR-PIT) differs from traditional PDT not only in the hydrophilicity of the photosensitizer, but also in its reliance on NIR light that has better tissue penetration than lower wavelength light. This new generation of antibody-photosensitizer conjugates (APC) demonstrates similar intravenous pharmacokinetics to naked antibodies, resulting in highly targeted tumor accumulation with minimal non target binding. When bound to targeted cells, APCs induce rapid, selective cytotoxicity after exposure to NIR light. Briefly, the photosensitizer, IRDye700DX, (IR700, a silica-phthalocyanine dye) is conjugated to a specific antibody customized to the expression profile of the tumor being treated. Then the APC is activated by exposure to NIR light at 690 nm, killing only APC-bound target cells. *In vitro* studies have demonstrated that NIR-PIT is highly target cell-specific, therefore, non-target expressing cells suffer no toxic effects (8). Recent data suggests that once the APC binds to the target cell and is exposed to NIR light, cell necrosis is rapid and irreversible due to structural damage to the cell membrane. For instance, cell membrane rupture can be demonstrated within minutes of exposure to NIR light in targeted cells (8–12). However, so far, NIR-PIT is limited to tumors located relatively shallow from the surface that can be easily exposed to NIR light. In this study, we investigate the efficacy of NIR-PIT for treating disseminated peritoneal ovarian cancer in a mouse model.

Material and methods

Reagents

Water soluble, silicon-phthalocyanine derivative, IRDye 700DX NHS ester and IRDye 800CW NHS ester were obtained from LI-COR Bioscience (Lincoln, NE, USA). Panitumumab, a fully humanized IgG_2 mAb directed against EGFR, was purchased from Amgen (Thousand Oaks, CA, USA). Trastuzumab, 95% humanized IgG_1 mAb directed against HER2, was purchased from Genentech (South San Francisco, CA, USA). All other chemicals were of reagent grade.

Synthesis of IR700-conjugated trastuzumab or panitumumab, and IR800-conjugated trastuzumab

Conjugation of dyes with mAbs was performed according to previous reports (8,11,13). In brief, panitumumab or trastuzumab (1 mg, 6.8 nmol) was incubated with IR700 NHS ester (60.2 μg, 30.8 nmol) or IR800CW NHS ester (35.9 μg, 30.8 nmol) in 0.1 mol/L Na_2HPO_4 (pH 8.6) at room temperature for 1 hr. The mixture was purified with a Sephadex G50 column (PD-10; GE Healthcare, Piscataway, NJ, USA). The protein concentration was determined with Coomassie Plus protein assay kit (Thermo Fisher Scientific Inc, Rockford, IL, USA) by measuring the absorption at 595 nm with spectroscopy (8453 Value System; Agilent Technologies, Santa Clara, CA, USA). The concentration of IR700 or IR800 was measured respectively by absorption at 689 nm or 774 nm with spectroscopy to confirm the number of fluorophore molecules conjugated to each mAb. The synthesis was controlled so that an average of four IR700 molecules or two IR800 molecules were bound to a single antibody. We performed SDS-PAGE as a quality control for each conjugate as previously reported (13). We abbreviate IR700 conjugated to trastuzumab as tra-IR700, to panitumumab as pan-IR700 and IR800 conjugated to trastuzumab as tra-IR800.

Cell culture

HER2 and luciferase-expressing SKOV3-luc-D3 cells were newly purchased from Caliper LifeSciences (Hopkinton, MA, USA) for this project in April 2014 and were not tested in our place. To evaluate specific cell killing by PIT, Balb/3T3 (purchased from ATCC (Rockville, MD) in 2009 and frozen and stocked cells without passage were thawed in May 2014 for this project that were not tested in our place) cells stably transfected and expressing DsRed (3T3/DsRed) were used as negative controls (8). Cells were grown in RPMI 1640 (Life Technologies, Gaithersburg, MD, USA) supplemented with 10% fetal bovine serum and 1% penicillin/streptomycin (Life Technologies) in tissue culture flasks in a humidified incubator at 37°C at an atmosphere of 95% air and 5% carbon dioxide.

Spheroid culture

Spheroids were generated by the hanging drop method in which five thousand SKOV-luc cells were suspended in 50 μL medium and were then dispensed into 96 well plates (3D Biomatrix Inc, Ann Arbor, MI, USA) following manufacture's instructions (9, 12).

Flow Cytometry

Fluorescence from cells after incubation with pan-IR700 or tra-IR700 was measured using a flow cytometer (FACS Calibur, BD BioSciences, San Jose, CA, USA) and CellQuest software (BD BioSciences). SKOV-luc cells (1×10^5) were incubated with each APC for 6 hr at 37°C. To validate the specific binding of the conjugated antibody, excess antibody (50 μg) was used to block 0.5 μg of dye-antibody conjugates (11).

Fluorescence microscopy

To detect the antigen specific localization of IR700 conjugates, fluorescence microscopy was performed (IX61 or IX81; Olympus America, Melville, NY, USA). Ten thousand cells were seeded on cover-glass-bottomed dishes and incubated for 24 hr. Tra-IR700 was then

added to the culture medium at 10 μg/mL and incubated at 37°C for 6 hr. The cells were then washed with PBS; Propidium Iodide (PI)(1:2000)(Life Technologies) and Cytox Blue (1:500)(Life Technologies), were used to detect dead cells. For spheroid evaluation, SYTO Blue42 (1:500)(Life Technologies) was used to detect living cells within the spheroid. They were added into the media 30 min before the observation. The cells were then exposed to NIR light (2 J/cm^2) and serial images were obtained. The filter was set to detect IR700 fluorescence with a 590–650 nm excitation filter, and a 665–740 nm band pass emission filter.

3D reconstructions of the spheroids were obtained with a confocal laser microscope (LSM5 meta, Carl Zeiss, Jena, Germany) after incubation for 30 min with Hoechst 33342 (1:500) (Life Technologies), (14). Sections of spheroids were first fixed with 3.7% formaldehyde in PBS for 10 min at room temperature followed by embedding with OCT (SAKURA, Tokyo, Japan). Then, they were frozen at −80°C, and sliced at 10 μm with a cryotome (LEICA CM3050 S, Leica microsystems, Wetzlar, Germany)(15). Analysis of the images was performed with ImageJ software (http://rsb.info.nih.gov/ij/).

In vitro NIR-PIT

One hundred thousand cells were seeded into 24 well plates or ten million cells were seeded onto a 10 cm dish and incubated for 24 hr. Medium was replaced with fresh culture medium containing 10 μg/mL of tra-IR700 which was incubated for 6 hr at 37°C. After washing with PBS, phenol red free culture medium was added. Then, cells were irradiated with a NIR laser, which emits light at 685 to 695 nm wavelength (BWF5-690-8-600-0.37; B&W TEK INC., Newark, DE, USA). The actual power density of mW/cm^2 was measured with an optical power meter (PM 100, Thorlabs, Newton, NJ, USA).

Cytotoxicity/ Phototoxicity assay

The cytotoxic effects of NIR-PIT with tra-IR700 were determined by the luciferase activity and flow cytometric PI staining. For luciferase activity, 150 μg/mL of D-luciferin-containing media (Gold Biotechnology, St Louis, MO, USA) was administered to PBS-washed cells 6 hr after PIT, and analyzed on a bioluminescence imaging (BLI) system (Photon Imager; Biospace Lab, Paris, France). We evaluated luciferase activity *in vitro* at varying times after PIT (1, 3, 6, 24 hr). For the flow cytometric assay, cells were trypsinized 6 hr after treatment and washed with PBS. PI was added to the cell suspension (final 2 μg/mL) and incubated at room temperature for 30 min, prior to flow cytometry.

Animal and tumor models

All *in vivo* procedures were conducted in compliance with the Guide for the Care and Use of Laboratory Animal Resources (1996), US National Research Council, and approved by the local Animal Care and Use Committee. Six- to eight-week-old female homozygote athymic nude mice were purchased from Charles River (NCI-Frederick). During procedures, mice were anesthetized with isoflurane.

In order to determine tumor volume, three million SKOV-luc cells were injected subcutaneously in the right dorsum of the mice. The greatest longitudinal diameter (length)

and the greatest transverse diameter (width) were measured with an external caliper. Tumor volumes based on caliper measurements were calculated by the following formula; tumor volume = length × width^2 × 0.5 (8,11). Tumors reaching approximately 50 mm^3 in volume were selected for further experiments.

For BLI, D-luciferin (15 mg/mL, 200 μL) was injected intraperitoneally and the mice were analyzed with a Photon Imager for luciferase activity at day 6. Mice were selected for further study based on tumor size and bioluminescence.

To evaluate the disseminated peritoneal ovarian cancer mouse model, five million SKOV-luc cells in PBS (total 300 μL) were injected into the peritoneal cavity. Twenty-seven days later D-luciferin (15 mg/mL, 200 μL) was injected intraperitoneally and imaged with the Photon Imager for luciferase activity in the abdomen; mice with sufficient activity were selected for further study.

Characterization of the disseminated peritoneal ovarian cancer mouse model

Both the disseminated peritoneal model and the subcutaneous bilateral flank models received 100 μg of tra-IR700 or tra-IR800 intravenously. One day after injection, serial images were performed with a fluorescence imager (Pearl Imager) for detecting IR700/IR800 fluorescence, and with the Photon Imager for BLI. Images of the mice were obtained with an iphone5 (Apple Inc., Cupertino, CA, USA).

In vivo NIR-PIT

SKOV-luc right dorsum tumor xenografts were randomized into 4 groups of at least 10 animals per group for the following treatments: (1) no treatment (control); (2) NIR light exposure at 100 J/cm^2 only; (3) 100 μg of tra-IR700 i.v., no NIR light exposure; (4) 100 μg of tra-IR700 i.v., NIR light administered at 100 J/cm^2 on day 1 after injection. These therapies were performed only once at day 4 after cell implantation. Mice were monitored daily, and tumor volumes were measured three times a week until the tumor diameter reached 2cm, whereupon the mouse was euthanized with carbon dioxide.

For fluorescence image and BLI, mice images were acquired over time with a fluorescence imager (Pearl Imager) for detecting IR700 fluorescence, and Photon Imager for BLI. For analyzing BLI, ROI of similar size were placed over the entire tumor.

For evaluation of PIT effects in the disseminated peritoneal ovarian cancer mouse model, mice were randomized into 4 groups of 6 animals per group for the following treatments: (1) no treatment (control); (2) only NIR light exposure at 100 J/cm^2; (3) 100 μg of tra-IR700 i.v., no NIR light exposure; (4) 100 μg of tra-IR700 i.v., NIR light administered at 100 J/cm^2 on day 1 after injection transcutaneously. Serial fluorescence imaging and BLI were obtained.

Statistical Analysis

Data are expressed as means ± s.e.m. from a minimum of four experiments, unless otherwise indicated. Statistical analyses were carried out using a statistics program (GraphPad Prism; GraphPad Software, La Jolla, CA, USA). For multiple comparisons, a one-way analysis of

variance (ANOVA) with post test (Kruskal-Wallis test with post-test) was used. $p < 0.05$ was considered to indicate a statistically significant difference.

Results

Confirmation of expression profile of SKOV-luc cells

The fluorescence signals obtained with pan-IR700 and tra-IR700 with SKOV-luc cells were evaluated by FACS. After 6 hr incubation with either pan-IR700 or tra-IR700, SKOV-luc cells showed higher brightness with tra-IR700 than pan-IR700 (Fig. 1A). These signals were completely blocked by the addition of excess trastuzumab or panitumumab, suggesting specific binding and validating that the addition of the luciferase gene had not altered the cell expression profile (16). These data suggested that HER2 was the preferable target for NIR-PIT due to its higher expression; therefore, we selected tra-IR700 as the experimental agent for all subsequent experiments.

Microscopy of the effects of NIR-PIT

Serial fluorescence microscopy of SKOV-luc cells was performed before and after NIR-PIT. After exposure to NIR light (2 J/cm^2) cellular swelling, bleb formation and rupture of the lysosome were observed (Fig. 1B). Time-lapse image analysis showed acute morphologic changes in the cell membrane (Supplementary video 1) and fluorescence of PI indicating cell death (Supplementary video 2). Most of these cellular changes were observed within 60 min after light exposure, indicating rapid induction of necrotic cell death after NIR-PIT. No significant changes were observed in EGFR-negative 3T3 cells after exposure to NIR light, suggesting NIR-PIT induced no damage in non-target cells (Supplementary Fig. S1).

Evaluation of *in vitro* NIR-PIT effect

In order to quantitate the effect of *in vitro* NIR-PIT, we performed a cytotoxicity assay 6hr after NIR light irradiation using PI staining and luciferase activity. Based on incorporation of PI, the cell death percentage increased in a light dose dependent manner. No significant cytotoxicity was observed with NIR light exposure alone or with tra-IR700 alone (Fig. 1C). Luciferase activity showed significant decreases of relative light units (RLU) in NIR-PIT-treated cells (Fig. 1D). BLI also showed a decrease of luciferase activity in a light dose dependent manner (Fig. 1E). NIR-PIT caused less cell death at 1hr and 3hr after light exposure than at 6hr, suggesting NIR-PIT induced cytotoxicity in this cell line was slower to respond to NIR-PIT than other cell types which have been reported (Supplementary Fig. S2) (9,11). Collectively, these studies confirm that NIR-PIT causes necrotic cell death in a light dose dependent manner, and NIR-PIT induced tumor cell death can be monitored by BLI.

Evaluation of NIR-PIT in a 3D spheroid

The efficacy of *in vitro* NIR-PIT was also examined in 3D spheroids composed of SKOV-luc cells. Compared to conventional monolayer cultures, 3D spheroids are superior models of tumors (11,17,18). Spheroids achieved a maximum size of approximately 700-μm diameter (Fig. 2A and B). 3D confocal microscopy indicated that the spheroids were spherical with an almost smooth surface (Fig. 2C). Frozen sections revealed that the cells were found evenly dispersed throughout the spheroid (Fig. 2D).

To visualize and quantify both single-shot and repeated NIR-PIT in the 3D spheroid model, concurrent microscopy with multiple staining was performed (Fig. 2E and F). At 1 hr post-PIT, a physical swelling of the spheroid was observed (Fig. 2E). The outer layer of the spheroid was stained with PI, indicating cell death. Repeated NIR-PIT with repeated incubation with Tra-IR700 every day led to the complete eradication of tumor cells within the spheroids (Fig. 2F). Decreasing numbers of cells with live-cell-staining (SYTO) and increasing numbers of cells with dead-cell-staining (PI) were demonstrated. Quantification with luciferase activity confirmed these results (Fig. 2G), suggesting that NIR-PIT could induce acute necrotic tumor killing effects not only in 2D but also in 3D cell cultures, and repeated NIR-PIT was capable of killing all cells within the spheroid.

In vivo NIR-PIT reduces tumor volume and luciferase activity in flank xenograft model

After NIR-PIT, significant differences in tumor volume in the PIT group were detected compared with control groups (Supplementary Fig. S3). Tumor volume was reduced significantly in the PIT group compared with other control groups ((PIT group vs control group at day 10, *p = 0.0001 < 0.001)(PIT group vs light only group at day 10, *p = 0.009 < 0.01)(PIT group vs i.v. only group at day 10, *p = 0.0004 < 0.001), Kruskal-Wallis test with post-test).

The NIR-PIT treatment effect was confirmed with BLI and fluorescence both of which decreased (Fig. 3A and B, and Supplementary Fig. S4A). BLI of tumor in the control, light only and i.v. only groups showed a gradual increase in RLU due to tumor growth (Fig. 3B and C). In contrast, luciferase activity gradually decreased up to 4 days after NIR-PIT to as low as 20.3 (Fig. 3B and C). At day 3, 4 and 7, quantitative analysis showed significant decreases of RLU in the PIT group (n = 5 mice in each group, (PIT group vs light only group at day 3, *p = 0.0137 < 0.05)(PIT group vs control group at day 4, **p = 0.0237 < 0.05)(PIT group vs light only group at day 4, **p = 0.0385 < 0.05)(PIT group vs control group at day 7, ***p = 0.0301 < 0.05)(PIT group vs light only group at day 7, ***p = 0.0255 < 0.05), Kruskal-Wallis test with post-test). Taken together, dramatic decreases of tumor size and BLI after PIT indicates NIR-PIT induced massive cell death in the flank model, and correlation between real tumor size and BLI response to NIR-PIT.

Characterization of the disseminated peritoneal ovarian cancer mouse model with fluorescence and BLI

In order to determine the natural history of the disseminated peritoneal ovarian cancer mouse model, serial fluorescence imaging and BLI were performed. The implanted tumors demonstrated high activity with fluorescence imaging based on IR700 or IR800, but also high activity on BLI, which co-localized with each other (Fig. 4). These data suggest that disseminated peritoneal ovarian cancer mouse model with SKOV-luc cells was successfully established; intravenously injection of agent could reach the disseminated tumors.

In vivo NIR-PIT effect on luciferase activity in disseminated peritoneal ovarian cancer mouse model

In order to monitor targeted tumor cell killing induced by NIR-PIT, BLI was used after NIR-PIT in the disseminated peritoneal model (Fig. 5A). IR700 fluorescence decreased after NIR

light irradiation as previously reported (Fig. 5B and Supplementary Fig. S4B). Using BLI, the RLU in the abdomen gradually increased in control groups due to growing tumor. In contrast, the RLU in the abdomen decreased progressively up to 7 day in the treatment group, although it increased slightly at 14 day post-PIT (Fig. 5B and C). At 7 and 14 days, the luciferase activity of the tumor treated by NIR-PIT was significantly decreased (n = 6 mice in each group, (PIT group vs control group at day 7, *p = 0.0037 < 0.01)(PIT group vs light only group at day 7, *p = 0.0257 < 0.05)(PIT group vs control group at day 14, ***p = 0.0174 < 0.05)(PIT group vs light only group at day 14, ***p = 0.0331 < 0.05)(PIT group vs i.v. only group at day 14, ***p = 0.0133 < 0.05), Kruskal-Wallis test with post-test). Thus, NIR-PIT caused significant targeted tumor cell killing effect in this disseminated peritoneal ovarian cancer mouse model.

Discussion

In spite of high initial response rates to standard front-line treatments for ovarian cancer using cytoreductive surgical debulking followed by platinum- or taxane-based chemotherapy, tumors eventually relapse and frequently acquire drug-resistance in a large proportion of patients. In these patients, peritoneal tumor dissemination with ascites is a major cause of cancer-related morbidity and death (2,3). Even with currently recommended chemotherapies, the outcome for ovarian cancer patients with advanced stage is only 12% at 5 years (4,19). Therefore, new-targeted therapies that potentially improve patient outcomes are under investigation by many groups (20–24). Among them, a clinical trial of traditional PDT for peritoneal metastases demonstrated no significant objective responses or long-term tumor control due to its lack of tumor selectivity (25). We believe NIR-PIT may address this issue by allowing the hydrophilic photosensitizer to be brought in close proximity to the cell membrane by the conjugated antibody. This NIR-PIT is a promising candidate because the APC not only accumulated homogeneously in the disseminated peritoneal tumors after intravenous injection but also killed significant amounts of cancer in the peritoneal space after NIR light exposure. With this NIR-PIT, intraperitoneal injection of APC might be an alternative route of administration to treat the disseminated peritoneal tumors. APC can firstly bind to the surface of peritoneal disseminated tumors, then be absorbed through the peritoneum and recirculate within the tumor vessels. However, most peritoneally injected APCs will be taken up in the liver, where APCs are catabolized, after draining into the portal venous system after absorption through the peritoneum. Thus, there is a risk to lose a large amount of efficacy of the APC. Without systemic recirculation, APC can only reliably bind to cancer cells within 0.2 mm from the surface (26). Therefore, NIR-PIT with intravenous APC demonstrates more homogeneous micro-distribution than intraperitoneal administration. Further, not all tumors within the abdomen is within the peritoneum. For instance, the draining lymphatics commonly become occluded with malignancy and would not be well treated by intraperitoneal application alone.

Bioluminescence (BLI) using firefly luciferase was used as a primary outcome measure in this study. It is a well-established method of determining *in vivo* viability (27), because the BLI reaction requires both oxygen and ATP to actively transport the substrate luciferin and subsequently catalyze the photochemical reaction (28). Fluorescent proteins (FPs) are a potential alternative for monitoring tumor growth in vivo (29) and would have better

translatable potencial into clinic because FPs do not need additional injection of substrates. Fluorescence imaging using FPs is better direct and stable method for longitudinal monitoring therapeutic effects of photo-therapy (30) for days or weeks than the bioluminescence imaging, which is used in this study, because most of FPs are stable in solution for days in vitro and fluoresced before FPs are taken up and catabolized by macrophages in vivo (29). Therefore, fluorescence imaging has already been used for longitudinal monitoring of therapeutic effects of PIT (8). Since NIR-PIT induced necrotic cell death leads to the release of ATP, BLI is an appropriate biomarker for NIR-PIT effects for designing preclinical experiments in mouse models (31–33). Therefore, in this study we used BLI to monitor tumor cell death of both HER2 expressing subcutaneous tumor xenografts and disseminated peritoneal tumors, and successfully detected the dramatic decrease of BLI signals in response to NIR-PIT in both models. These data clearly demonstrate that NIR-PIT is a potential candidate for the treatment of disseminated peritoneal cancer, which expresses a target molecule.

There are several limitations to this study. First, not all ovarian cancers overexpress HER2, and therefore this particular target may not be ideal in other ovarian cancers. Therefore, we are currently investigating NIR-PIT against ovarian cancer by targeting mesothelin, which is reportedly another great target molecule expressing on ovarian cancers (34), and have been obtaining similar success (Supplementary Fig. S5). Fortunately, NIR-PIT has proven effective with almost all APCs with which it has been attempted and therefore, it is promising that the proper APC or combination of APCs could be found to treat a specific phenotype of ovarian cancer cell membrane expression (15). We were also unable to determine long-term side effects of NIR-PIT in this limited model. Short-term studies of the mice demonstrated no apparent adverse events after NIR-PIT. It is possible that sudden widespread cell necrosis could cause toxicity both acutely and delayed but none was observed in this model. Additionally, it is clear that NIR-PIT alone will not be sufficient to treat disseminated intraperitoneal ovarian cancer, although the use of NIR light in to activate IR700 will produce deeper tissue penetration within larger masses than the shorter wavelengths of light needed for PDT photoactivation or other phototherapy using UV light irradiation (35). Therefore, we foresee NIR-PIT as an adjuvant to surgery with an initial debulking procedure followed by NIR-PIT to “mop up” residual disease. Furthermore, it is interesting to consider the possibility that systemic chemotherapy may be more effective after NIR-PIT and surgery than surgery alone. Previous studies have shown that NIR-PIT results in heightened deposition of systemically administered nano-sized drugs within the treated tumor due to the preservation of tumor vessels with increased vascular permeability because intravenously administered APC specifically accumulated in cancer cells adjacent to tumor vessels. Therefore, current or future chemotherapies for ovarian cancer may benefit from prior treatment with NIR-PIT (13).

In addition to the critical pharmacokinetic differences between traditional PDT and NIR-PIT, there are significant pharmacodynamic differences as well. Conventional PDT relies mostly on the type 2 oxidation reaction, and therefore, requires sufficient oxygen concentrations at the treatment site. Our results and others demonstrate that cytotoxicity induced by NIR-PIT does not totally rely on oxygen concentration or the existence of singlet oxygen quenchers (36). Furthermore, cytotoxicity induced by NIR-PIT is primarily within

the cell membrane rather within the mitochondria as occurs with conventional PDT. Therefore, both pharmacokinetics of the APC and pharmacodynamics of the photosensitizer are different between traditional PDT/PIT and NIR-PIT.

In conclusion, this study shows the feasibility of NIR-PIT for effectively treating disseminated peritoneal ovarian cancer in a mouse model. This treatment approach represents a new method of potentially treating ovarian cancer as an adjuvant to existing therapies such as surgery and chemotherapy.

Supplementary Material

Refer to Web version on PubMed Central for supplementary material.

Acknowledgments

To perform this research, we (Kazuhide Sato, Hirofumi Hanaoka, Rira Watanabe, Takahito Nakajima, Peter L. Choyke, Hisataka Kobayashi) were supported by the Intramural Research Program of the National Institutes of Health, National Cancer Institute, Center for Cancer Research. Kazuhide Sato is supported with JSPS Research Fellowship for Japanese Biomedical and Behavioral Researchers at NIH.

Disclosure statement

NIH/DHHS holds a patent on photoimmunotherapy

References

1. Siegel R. Cancer statistics, 2013. CA cancer J Clin. 2013; 63:11–30. [PubMed: 23335087]
2. Ng JS, Low JJH, Ilancheran a. Epithelial ovarian cancer. Best Pract Res Clin Obstet Gynaecol. 2012; 26:337–345. [PubMed: 22281513]
3. Society MM. PATIENTS WITH STAGE III AND STAGE IV OVARIAN CANCER. N Engl J Med. 1996; 334:1–6. [PubMed: 7494563]
4. Sudo T. Molecular-targeted therapies for ovarian cancer: prospects for the future. Int J Clin Oncol. 2012; 17:424–429. [PubMed: 22915194]
5. Banerjee S, Kaye S. The role of targeted therapy in ovarian cancer. Eur J Cancer. 2011; 47(Suppl 3):S116–S130. [PubMed: 21943965]
6. Mew D, Wat C, Towers GHN, Levy JG. PHOTOIMMUNOTHERAPY : TREATMENT OF ANIMAL TUMORS WITH TUMOR-SPECIFIC. J Immunol. 1983; 130:1473–1477. [PubMed: 6185591]
7. Spring BQ, Abu-Yousif AO, Palanisami A, Rizvi I, Zheng X, Mai Z, et al. Selective treatment and monitoring of disseminated cancer micrometastases in vivo using dual-function, activatable immunoconjugates. Proc Natl Acad Sci U S A. 2014; 111:E933–E942. [PubMed: 24572574]
8. Mitsunaga M, Ogawa M, Kosaka N, Rosenblum LT, Choyke PL. Cancer cell – selective in vivo near infrared photoimmunotherapy targeting specific membrane molecules. Nat Med. 2011; 17:1685–1691. [PubMed: 22057348]
9. Mitsunaga M, Nakajima T. Immediate in vivo target-specific cancer cell death after near infrared photoimmunotherapy. BMC Cancer. 2012; 12:1. [PubMed: 22212211]
10. Mitsunaga M, Nakajima T, Sano K, Choyke PL, Kobayashi H. Near-infrared Theranostic Photoimmunotherapy (PIT): Repeated Exposure of Light Enhances the Effect of Immunoconjugate. Bioconjug Chem. 2012; 23:604–609. [PubMed: 22369484]
11. Sato K, Watanabe R, Hanaoka H, Harada T, Nakajima T, Kim I, et al. Photoimmunotherapy: Comparative effectiveness of two monoclonal antibodies targeting the epidermal growth factor receptor. Mol Oncol. 2014; 8:620–632. [PubMed: 24508062]

12. Nakajima T, Sano K, Mitsunaga M, Choyke PL, Kobayashi H. Real-time monitoring of in vivo acute necrotic cancer cell death induced by near infrared photoimmunotherapy using fluorescence lifetime imaging. Cancer Res. 2012; 72:4622–4628. [PubMed: 22800710]
13. Sano K, Nakajima T, Choyke PL, Kobayashi H. Markedly Enhanced Permeability and Retention Effects Induced by Photo-immunotherapy of Tumors. ACS Nano. 2013; 7:717–724. [PubMed: 23214407]
14. Sato K, Watanabe T, Wang S, Kakeno M, Matsuzawa K, Matsui T, et al. Numb controls E-cadherin endocytosis through p120 catenin with aPKC. Mol Biol Cell. 2011; 22:3103–3119. [PubMed: 21775625]
15. Nakajima T, Sano K, Choyke PL, Kobayashi H. Improving the efficacy of Photoimmunotherapy (PIT) using a cocktail of antibody conjugates in a multiple antigen tumor model. Theranostics. 2013; 3:357–365. [PubMed: 23781283]
16. Gaborit N, Larbouret C, Vallaghe J, Peyrusson F, Bascoul-Mollevi C, Crapez E, et al. Time-resolved fluorescence resonance energy transfer (TR-FRET) to analyze the disruption of EGFR/HER2 dimers: a new method to evaluate the efficiency of targeted therapy using monoclonal antibodies. J Biol Chem. 2011; 286:11337–11345. [PubMed: 21282108]
17. Dubessy C, Merlin JM, Marchal C, Guillemin F. Spheroids in radiobiology and photodynamic therapy. Crit Rev Oncol Hematol. 2000; 36:179–192. [PubMed: 11033305]
18. Graff CP, Wittrup KD. Theoretical analysis of antibody targeting of tumor spheroids: importance of dosage for penetration, and affinity for retention. Cancer Res. 2003; 63:1288–1296. [PubMed: 12649189]
19. Smolle E, Taucher V, Haybaeck J. Malignant ascites in ovarian cancer and the role of targeted therapeutics. Anticancer Res. 2014; 34:1553–1561. [PubMed: 24692682]
20. Morotti M, Becker CM, Menada MV, Ferrero S. Targeting tyrosine-kinases in ovarian cancer. Expert Opin Investig Drugs. 2013; 22:1265–1279.
21. Pliarchopoulou K, Pectasides D. Epithelial ovarian cancer: focus on targeted therapy. Crit Rev Oncol Hematol. 2011; 79:17–23. [PubMed: 20674385]
22. Penzvalto Z, Surowiak P, Gyorffy B. Biomarkers for systemic therapy in ovarian cancer. Curr Cancer Drug Targets. 2014; 14:259–273. [PubMed: 24605893]
23. Weberpals JI, Koti M, Squire J a. Targeting genetic and epigenetic alterations in the treatment of serous ovarian cancer. Cancer Genet. 2011; 204:525–535. [PubMed: 22137482]
24. Sheppard KE, Cullinane C, Hannan KM, Wall M, Chan J, Barber F, et al. Synergistic inhibition of ovarian cancer cell growth by combining selective PI3K/mTOR and RAS/ERK pathway inhibitors. Eur J Cancer. 2013; 49:3936–3944. [PubMed: 24011934]
25. Hahn SM, Fraker DL, Mick R, Metz J, Busch TM, Smith D, et al. A phase II trial of intraperitoneal photodynamic therapy for patients with peritoneal carcinomatosis and sarcomatosis. Clin Cancer Res. 2006; 12:2517–2525. [PubMed: 16638861]
26. Kosaka N, Ogawa M, Paik DS, Paik CH, Choyke PL, Kobayashi H. Semiquantitative assessment of the microdistribution of fluorescence-labeled monoclonal antibody in small peritoneal disseminations of ovarian cancer. Cancer Sci. 2010; 101:820–825. [PubMed: 19961490]
27. Contag PR, Olomu IN, Stevenson DK CC. Bioluminescent indicators in living mammals. Nat Med. 1998; 4:245–247. [PubMed: 9461201]
28. Dothager RS, Flentie K, Moss B, Pan M-H, Kesarwala A, Piwnica-Worms D. Advances in bioluminescence imaging of live animal models. Curr Opin Biotechnol. 2009; 20:45–53. [PubMed: 19233638]
29. Hoffman RM. The multiple uses of fluorescent proteins to visualize cancer in vivo. Nat Rev Cancer. 2005; 5:796–806. [PubMed: 16195751]
30. Matsumoto Y, Miwa S, Zhang Y, Hiroshima Y, Yano S, Uehara F, et al. Efficacy of tumor-targeting salmonella typhimurium A1-R on nude mouse models of metastatic and disseminated human ovarian cancer. J Cell Biochem. 2014; 115:1996–2003. [PubMed: 24924355]
31. Zamaraeva MV, Sabirov RZ, Maeno E, Ando-Akatsuka Y, Bessonova SV, Okada Y. Cells die with increased cytosolic ATP during apoptosis: a bioluminescence study with intracellular luciferase. Cell Death Differ. 2005; 12:1390–1397. [PubMed: 15905877]

32. Rehemtulla A, Stegman LD, Cardozo SJ, Gupta S, Hall DE, Contag CH, et al. Rapid and Quantitative Assessment of Cancer Treatment Response Using In Vivo Bioluminescence Imaging 1 Days post sham treatment. Neoplasia. 2000; 2:491–495. [PubMed: 11228541]

33. Leist BM, Single B, Castoldi AF, Kühnle S. A Switch in the Decision Between Apoptosis and Necrosis. J Exp Med. 1997; 185:1481–1486. [PubMed: 9126928]

34. Pastan I, Hassan R. Discovery of Mesothelin and Exploiting It as a Target for Immunotherapy. Cancer Res. 2014:2907–2912. [PubMed: 24824231]

35. Hiroshima Y, Maawy A, Zhang Y, Sato S, Murakami T, Yamamoto M, et al. Fluorescence-guided surgery in combination with UVC irradiation cures metastatic human pancreatic cancer in orthotopic mouse models. PLoS One. 2014; 9:e99977. [PubMed: 24924955]

36. Shirasu N, Yamada H. Potent and specific antitumor effect of CEA-targeted photoimmunotherapy. Int J Cancer. 2014:1–14.

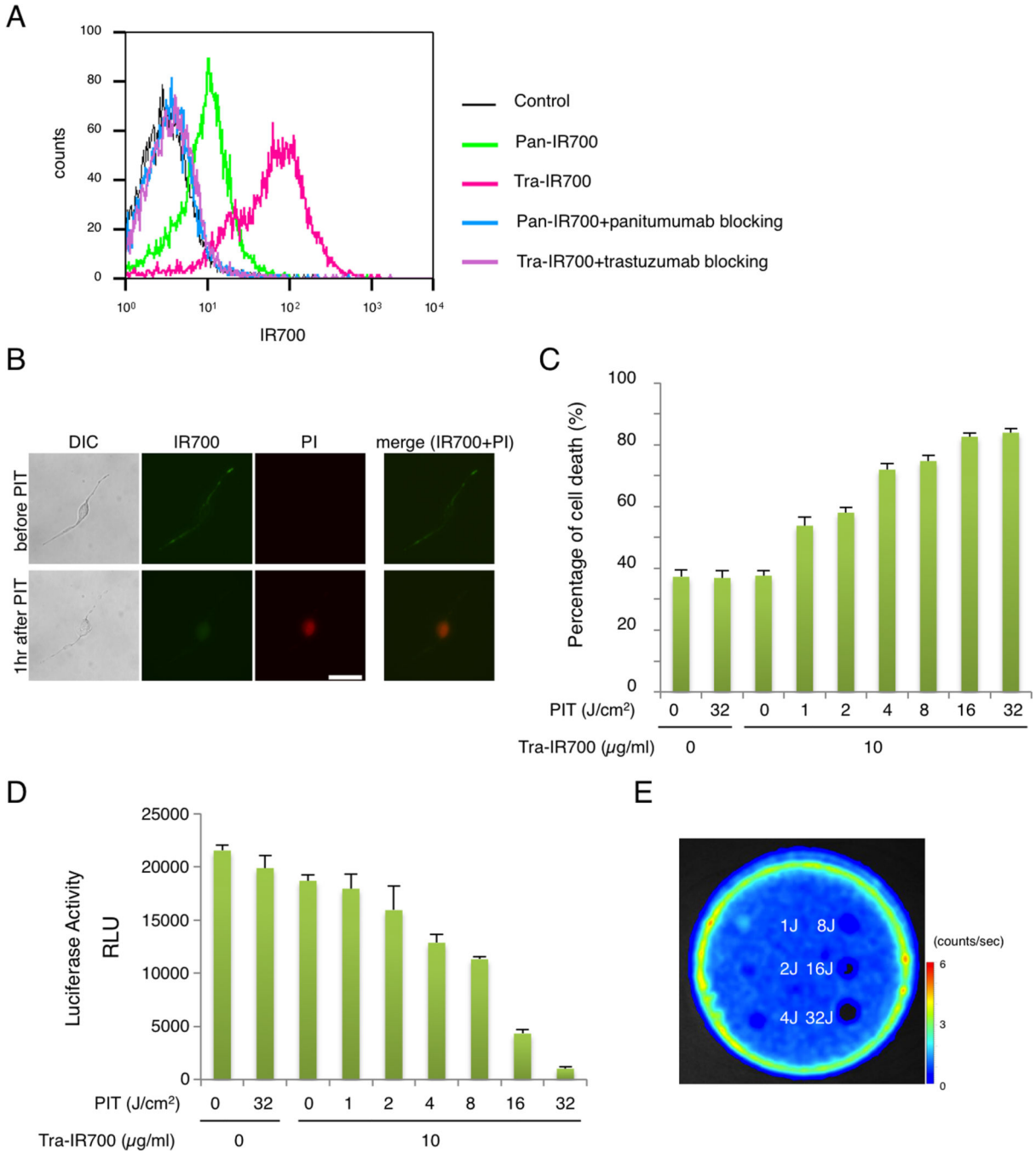

Figure 1. Confirmation of HER2 expression as a target for NIR-PIT in SKOV-luc cells

(A) Expression of HER1 and HER2 in SKOV-luc cells was examined with FACS. HER2 was overexpressed more than HER1. Specific binding was demonstrated with a blocking study. (B) SKOV-luc cells were incubated with tra-IR700 for 6 hr, and observed with a microscope before and after irradiation of NIR light (2 J/cm^2). Necrotic cell death was observed after exposure to NIR light (1 hr after PIT). Bar = 50 μm. (C) Membrane damage and necrosis induced by NIR-PIT was measured by dead cell count using PI staining. Cell killing increased in a NIR-light dose-dependent manner. (D) Luciferase activity in SKOV-

luc cells was measured as relative light unit (RLU), which also decreased in a NIR-light dose-dependent manner. (E) Bioluminescence imaging (BLI) of a 10 cm dish demonstrated that luciferase activity in SKOV-luc cells decreased in a NIR-light dose-dependent manner.

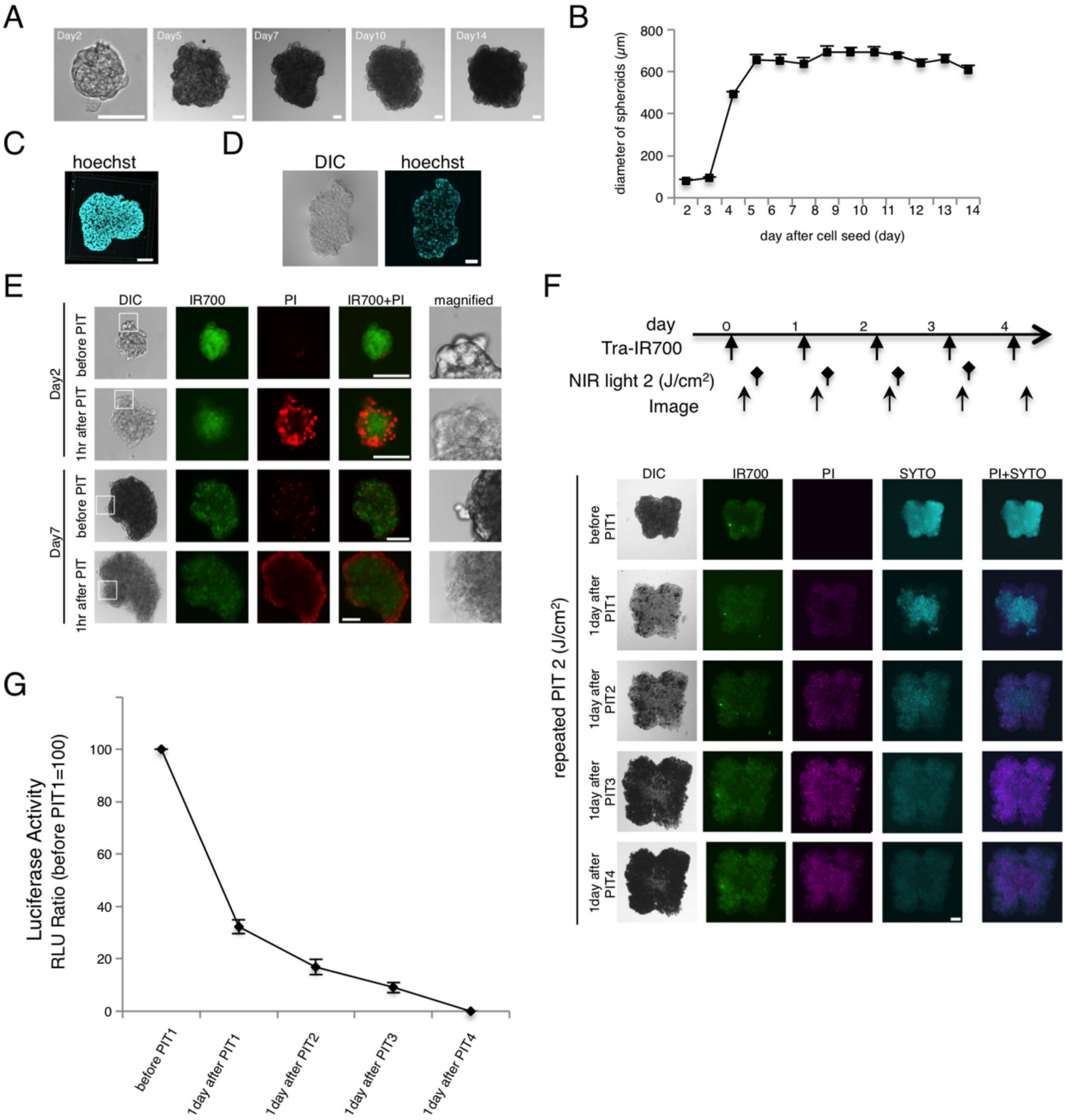

Figure 2. Characterization of NIR-PIT in 3D spheroids

(A) Representative image of SKOV-luc 3D spheroid. Bar = 100 μm. (B) 3D spheroids grew to around 700 μm. (C) 3D reconstruction image of 3D spheroid at day 7. Bar = 100 μm. (D) Frozen section of 3D spheroid. Cells accumulate within the core of the spheroid. Bar = 100 μm. (E) 3D spheroid at day 2 and day 7 after 6hr incubation with tra-IR700, before and after irradiation of NIR light (2 J/cm^2). Necrotic cell death was observed 1hr after NIR light. Bar = 100 μm. (F) 3D spheroid at day 7 treated by repeated NIR-PIT (2 J/cm^2). Bar = 100 μm. SYTO staining was used for detection of living cells. The treatment regimen is shown above

the images. (G) Luciferase activity in 3D spheroids gradually decreased after repeated NIR-PIT leading to complete killing of cells in the spheroid (n = 10).

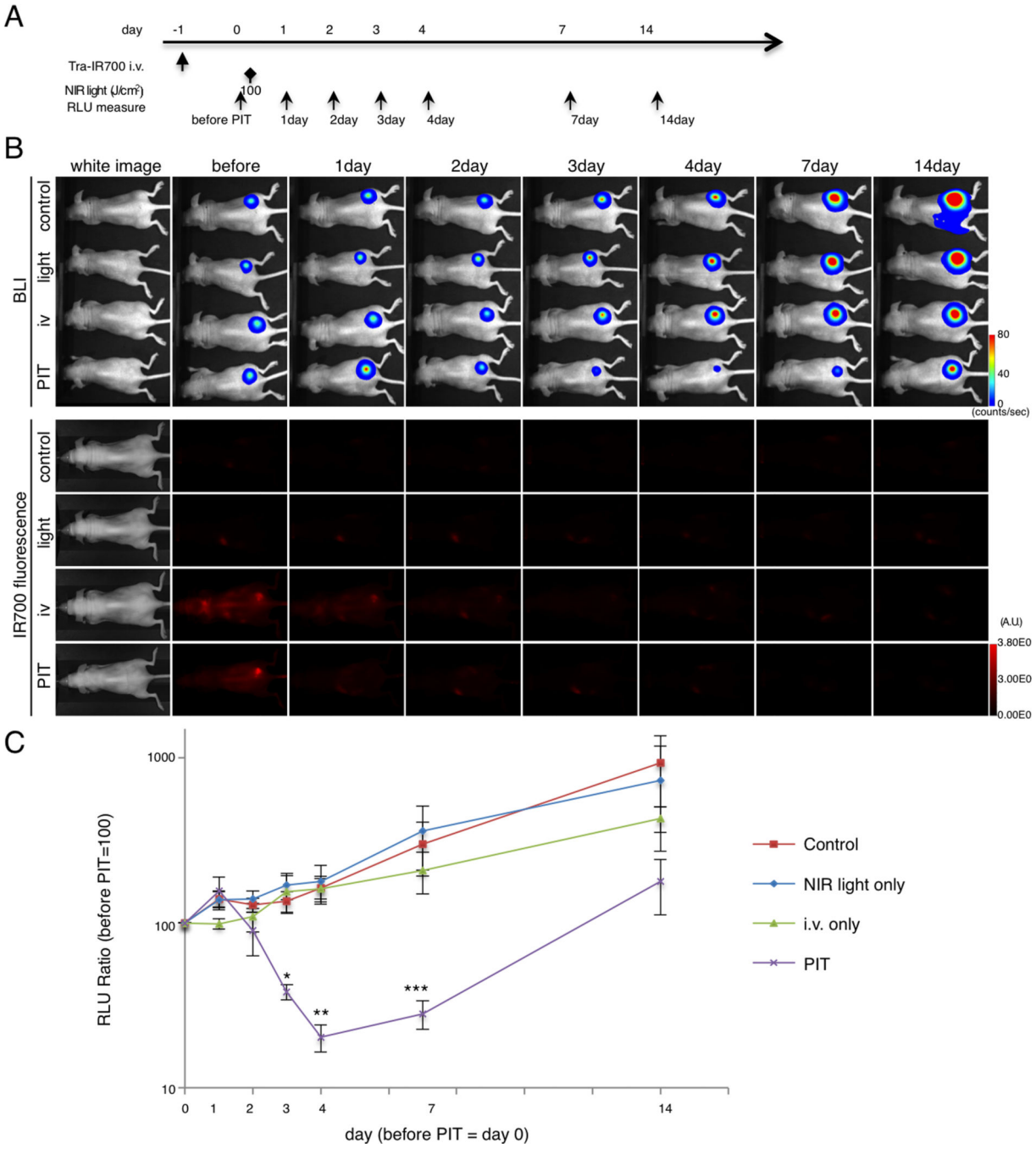

Figure 3. Evaluation of NIR-PIT by luciferase activity in flank model

(A) The regimen of NIR-PIT is shown. Images were obtained at each time point as indicated. (B) *In vivo* BLI and fluorescence imaging of tumor bearing mice in response to NIR-PIT. Prior to NIR-PIT, tumors were approximately the same size and exhibited similar bioluminescence. (C) Quantitative RLU showed a significant decrease in PIT-treated tumors (n = 5 mice in each group (PIT group vs light only group at day 3, *p = 0.0137 < 0.05)(PIT group vs control group at day 4, **p = 0.0237 < 0.05)(PIT group vs light only group at day 4, **p = 0.0385 < 0.05)(PIT group vs control group at day 7, ***p = 0.0301 < 0.05)(PIT

group vs light only group at day 7, ***p = 0.0255 < 0.05), Kruskal-Wallis test with post-test).

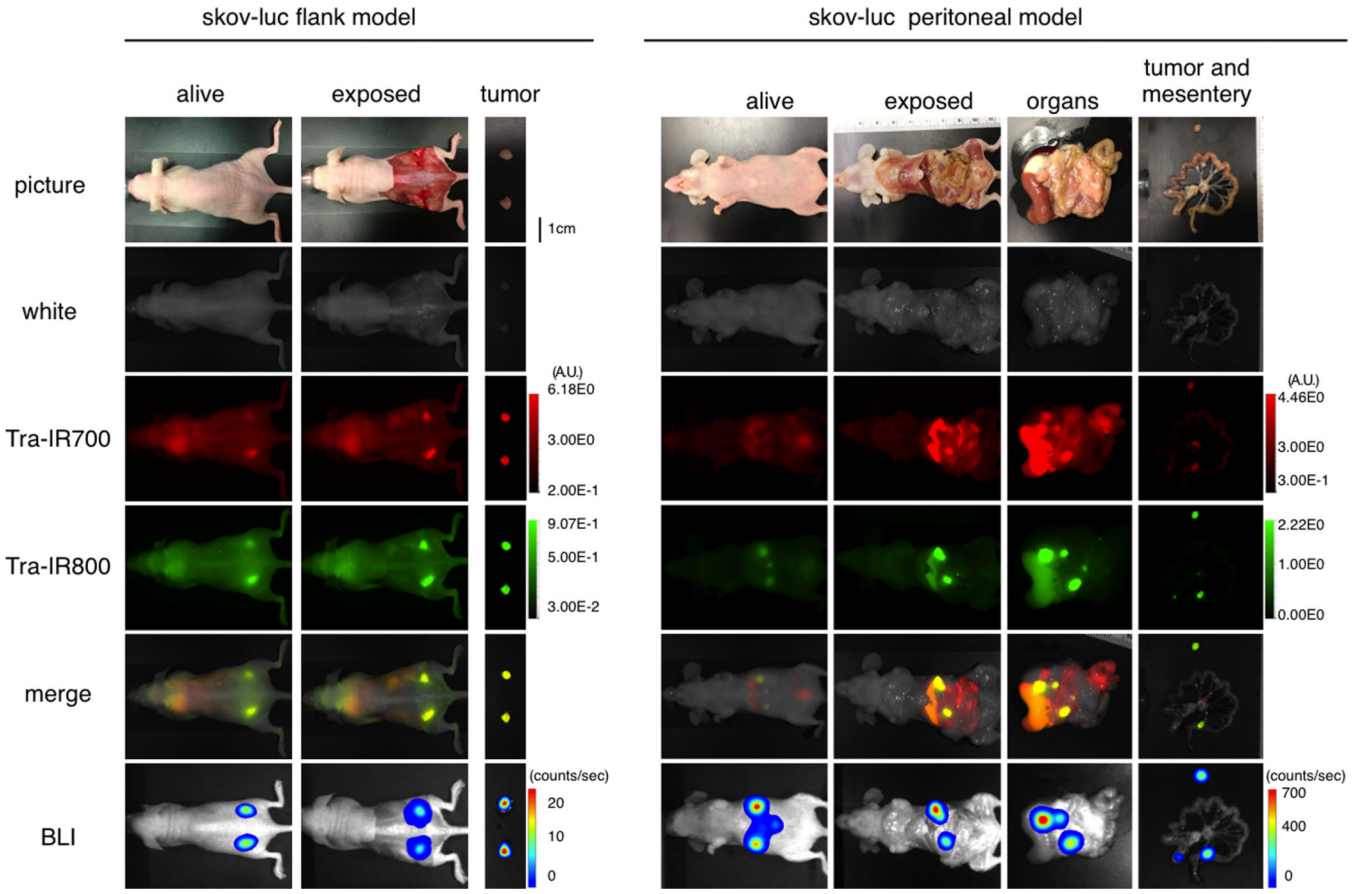

Figure 4. Characterization the disseminated peritoneal tumor model

In vivo BLI and fluorescence imaging of SKOV-luc tumor in flank and peritoneal model are shown and indicated colocalization of signal. To avoid auto-fluorescence from the intestine, Tra-IR800 was used as well as Tra-IR700 for imaging.

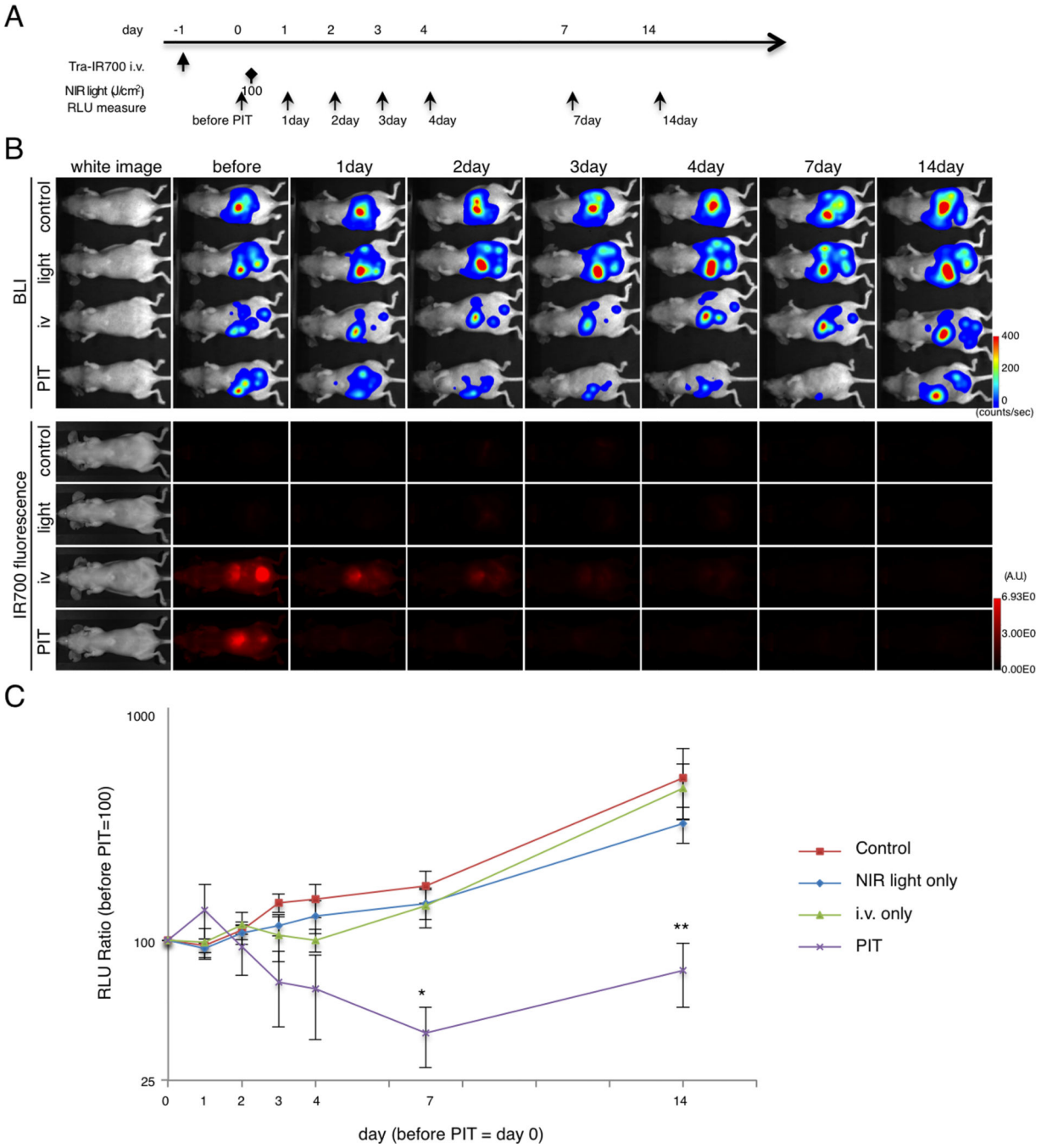

Figure 5. Evaluation of NIR-PIT effects in disseminated peritoneal model

(A) The regimen of NIR-PIT is shown. Images were obtained at each time point as indicated. (B) *In vivo* BLI and fluorescence imaging of disseminated peritoneal model. Prior to treatment mice exhibiting approximately the same luciferase activity in the abdomen were selected. (C) Quantitative RLU in the disseminated peritoneal model showed a significant decrease at day 7 and day 14 in the PIT (n = 6 mice in each group, (PIT group vs control group at day 7, *p = 0.0037 < 0.01)(PIT group vs light only group at day 7, *p = 0.0257 < 0.05)(PIT group vs control group at day 14, ***p = 0.0174 < 0.05)(PIT group vs light only

group at day 14, ***p = 0.0331 < 0.05)(PIT group vs i.v. only group at day 14, ***p = 0.0133 < 0.05), Kruskal-Wallis test with post-test).